

1 **Effect of three pillars on hydrological model calibration: data length, spin-up**
2 **period and spatial model resolution**

3 **Ömer Ekmekcioğlu^{1*}, Mehmet Cüneyd Demirel¹, Martijn J. Booij²**

4 ¹ Department of Civil Engineering, Istanbul Technical University, 34469 Maslak, Istanbul,
5 Turkey.

6 ² Water Engineering and Management, Faculty of Engineering Technology, University of
7 Twente, Enschede 7500 AE, The Netherlands

8 Corresponding author: Ömer Ekmekcioğlu (omer.ekmekcioglu@itu.edu.tr)

9

10 **Key Points:**

- 11 • A systematic approach is presented to identify appropriate calibration data length, spin-up
12 period and spatial model resolution
- 13 • Dependency of model performance on data length, spin-up period and spatial resolution
14 of the model schematization is revealed for the Moselle River
- 15 • Three user-defined pillars in modelling should not be overlooked due to trade-off
16 between computational costs and model performance

17

18 **Abstract**

19 In general, calibration of a hydrologic model is essential to better simulate the basin processes
20 and behaviour by fitting the model simulated fluxes to observed fluxes. A major challenge in the
21 calibration process is to choose the appropriate length of the observed data series and spatio-
22 temporal resolution of the model schematization. We present a multi-case calibration approach
23 for determining three pillars of an optimum hydrological model configuration: calibration data
24 length, spin-up period and spatial resolution of the hydrological model. The approach is
25 evaluated for the Moselle River basin using calibration and validation results from the spatially
26 distributed meso-scale Hydrological Model (mHM) for 105 different cases representing the
27 combinations of three calibration data lengths, seven spin-up periods and five spatial model
28 resolutions. A metaheuristic global optimization method, i.e. Dynamically Dimensioned Search
29 (DDS) algorithm, and a well-known hydrological performance metric, i.e. Nash Sutcliffe
30 Efficiency (NSE), are utilized for each of the 105 calibration cases. The results show that a 10-
31 year calibration data length, 2-year spin-up period and a 4 km model resolution are appropriate
32 for the Moselle basin to reduce the computational burden. Analyzing the combined effects
33 further allowed us to understand the interactions of these three usually overlooked pillars in
34 hydrological modeling.

35 **1 Introduction**

36 Hydrological models are crucial tools to evaluate physical processes and quantify water
37 balance components in a catchment. They can be classified according to the amount of physics
38 incorporated as empirical (or data-driven), conceptual and physically-based models. The focus in
39 this study is on physically-based regarding the amount of physics and fully-distributed regarding
40 the spatial resolution of the models. Obviously, the choice of the model type together with data

41 availability such as the spatial resolution of inputs, the length of the spin-up period and the
42 parameter calibration strategy all affect the model performance (Blöschl & Sivapalan, 1995). The
43 determination of all these aspects in a calibration framework is related to appropriate modeling in
44 hydrology and should be based on the modeling objective, data availability and a systematic
45 analysis of the model-catchment interaction (Booij, 2005). We focus on user-defined options in
46 hydrological modelling as we are interested in identifying the appropriate calibration data length,
47 spin-up period and spatial model resolution in the Moselle River basin.

48 The calibration process, which has utmost importance to minimize the parameter
49 uncertainty (Sreedevi & Eldho, 2019; Westerberg et al., 2020), is described as the optimization
50 of uncertain parameter values in the model to obtain sufficient accuracy in model outcomes
51 (Simunek et al., 2012). Since calibration can be performed by trial-and-error for different
52 conditions, i.e. manual calibration (Gelleszun et al., 2017), and also with mathematical
53 algorithms, i.e. automatic calibration (Madsen, 2003), time-efficiency is a major challenge. The
54 main constraint in determining the calibration period is the availability of data, i.e. long time-
55 series of runoff or other model output or state variables (Sorooshian et al., 1997). In general,
56 using 20-year data for the calibration period is assumed to be sufficient for large basins to
57 account for climatological and hydrological variability (Epstein et al., 1998). Although data
58 records for large basins might be available for more than 30 years, keeping the calibration period
59 as long as possible is computationally inefficient and not always meaningful, in particular when
60 climatic or other trends are present in the time series and the model only should be calibrated on
61 the most representative (i.e. most recent) time period (Daggupati et al., 2015). For instance,
62 Perrin et al. (2007) found that a much smaller number of random days (~300 days) is sufficient
63 for calibration of models with a small number of parameters.

64 In different studies, even data periods of 10 years or less have been used considering both
65 computational resources and limited data availability (Andersen et al., 2001; Kim et al., 2018).
66 Zheng et al. (2018) analyzed the impact of different calibration periods on model results using
67 data-driven techniques. They concluded that the model performance may increase by considering
68 temporal variability and extreme events in the calibration process. In addition, a number of
69 studies has confirmed that quality of data increases calibration performance in distributed
70 hydrological models (Beck et al., 2017; Herman et al., 2018; Näschen et al., 2018). Raihan et al.
71 (2020) evaluated the calibration performance of hydrological models according to different
72 performance criteria and showed that the simulations were not considerably successful
73 particularly for extreme low flows due to the limited temporal variability and poor data quality of
74 the calibration data.

75 Another factor affecting the calibration performance of hydrological models is the length
76 of the spin-up period, which provides the required initial model state (Yang et al., 1995). The
77 required spin-up period highly depends on the input data of the catchment and the hydrological
78 response (Rodell et al., 2005). In addition, determining the optimum spin-up period is essential,
79 since both shorter and longer spin-up periods may have negative effects on the calibration
80 performance. A shorter spin-up period inevitably leads to a low (even wrong) performance
81 evaluation, whereas a longer spin-up period can lead to a waste of the data and misinterpretation
82 of the results (Ajami et al., 2014). Practitioners generally consider the first two or three years as
83 acceptable as spin-up period depending on the model structure. There have been studies using
84 only a spin-up period of one year for lumped models (Rahman et al., 2016), semi-distributed
85 models (Abdo et al., 2009; Xu et al., 2013) and distributed models (Cuo et al., 2006; Lohmann et
86 al., 1998; Revilla-Romero et al., 2016). Although there is common sense that the spin-up period

87 varies from one year to several years up to ten years (Shi et al., 2008), no consensus has been
88 reached in this regard (Kim et al., 2018). Sood et al. (2013) performed simulations with a
89 monthly time step, since they had monthly streamflow observations, and the first two years of a
90 13-year data period have been used as spin-up period, while the remaining 11 years have been
91 utilized for model calibration. Ashraf (2013) performed simulations on a monthly basis as well
92 and divided the entire data set into two periods with six years as spin-up period and ten years as
93 calibration period. With a few exceptions, studies conducted to identify the optimum spin-up
94 period surprisingly did not attract the research community's attention, particularly for physically-
95 based distributed hydrological models.

96 Besides, heterogeneous land surface conditions require a sufficiently long spin-up period
97 (Shrestha & Houser, 2010). Ajami et al. (2014) emphasize the importance of a multi-criteria
98 approach, which includes the groundwater storage, unsaturated zone storage, depth to water
99 table, root zone storage, discharge, snow water equivalent and energy fluxes, in determining the
100 spin-up period of integrated hydrological models. The length of spin-up periods also depends on
101 the initial soil moisture content, soil depth, soil and vegetation type and groundwater storage at
102 the start of the simulations, in addition to the temperature and rainfall forcings (Cosgrove et al.,
103 2003). With a method based on relative changes in monthly groundwater storages, Ajami et al.
104 (H. Ajami et al., 2014) presented a hybrid approach on the basis of integration of ParFlow, which
105 is an integrated hydrological model, and the empirical depth-to-water-table function, to satisfy
106 state equilibrium conditions. They reduced the spin-up period by approximately 50% (from 20
107 years to 10-12 years) compared to the conventional continuous recursive simulation approach,
108 which is widely employed for the determination of spin-up periods in land surface models.

109 Regardless of the model complexity, another issue which has a significant impact on
110 hydrological model performance is the spatial model resolution (Koren et al., 1999). The spatial
111 resolution to be used in a model is not only related to the availability of meteorological input
112 data but also to the computational resources (Sood & Smakhtin, 2015). Accordingly, simulation
113 performance may either increase or decrease depending on the spatial resolution (Booij, 2002;
114 2005; Bucchignani et al., 2016; Pang et al., 2020). However, in some cases, a considerable
115 change is not observed indicating that the model structure is suitable for all resolutions (Merz et
116 al., 2009). In addition, the spatial variability of storm events also has an influence on the
117 appropriate spatial resolution of the model. Lumped models may perform accurately with a
118 spatially uniform input distribution, while they may need a higher spatial resolution (e.g. sub-
119 basins) in the case of a non-uniform spatial input distribution (Tian et al., 2020). Pang et al.
120 (Pang et al., 2020) evaluated the precipitation model input, both temporally and spatially, based
121 on the differences of various open access precipitation products.. In semi-distributed conceptual
122 models, the spatial resolution is determined based on the sub-basin distribution. Distributed
123 models provide distributed outputs since spatial heterogeneity is taken into account (Dehotin &
124 Braud, 2008). Etchevers et al. (2001) performed simulations for spatial resolutions of 1 km, 8 km
125 and 46 km using the soil-vegetation-atmosphere transfer (SVAT) model. They obtained
126 mediocre simulation results for the 46 km resolution, whereas flash-flood events were better
127 captured in the model with a 8 km resolution. Chen et al. (2017) employed the Liuxihe model,
128 i.e. a physically based distributed hydrological model, to investigate flood events in Liujiang
129 River basin, China, which covers an area of about 60000 km². They calibrated the model using
130 Particle Swarm Optimization (PSO) for a total of 29 flood events. Considering five different
131 spatial model resolutions, i.e. 200, 400, 500, 600 and 1000 m, they concluded that the results for

132 the 1 km grid were not meaningful. The peak values were captured when applying resolutions of
133 500 m or smaller. Although slightly better results were obtained for 400 m, they chose 500 m
134 grids as the appropriate spatial resolution considering the computational burden. Fully distributed
135 models are more sensitive to resolution of the rainfall input as compared to semi-distributed
136 models (Gires et al., 2015). Most of the current studies investigated either the effects of the
137 model input resolution or the spin-up period on the model results. No study is known to the
138 authors which explicitly assesses the effects of the spatial resolution of the model together with
139 the length of the spin-up period and calibration period on the model performance.

140 We aim to comprehensively investigate the impact of the three major but overlooked
141 pillars, (1) calibration period, (2) spin-up period and (3) spatial model resolution, on the
142 calibration and validation performance of a physically-based distributed hydrological model for
143 the Moselle River basin in France and Germany. The study area and data are introduced in
144 section 2. The model and calibration framework are presented in section 3. The calibration and
145 validation results are presented and discussed in sections 4 and 5. Finally, the key conclusions
146 are drawn in Section 6.

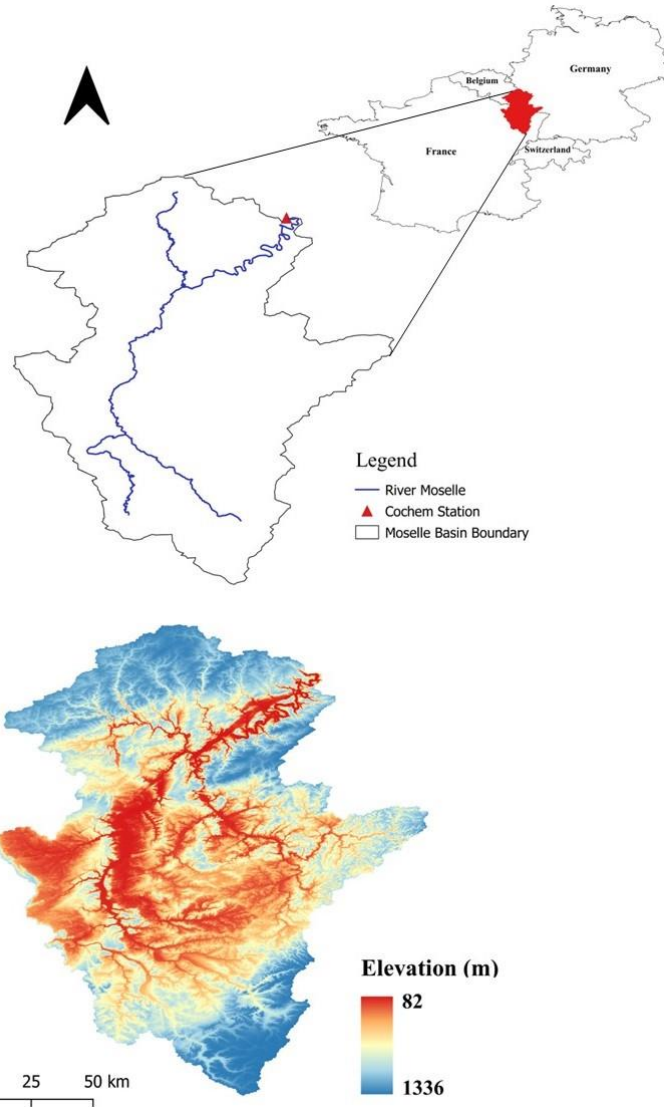
147 **2 Study Area and Data**

148 2.1 Study area

149 The focus of this study is the Moselle River basin (Figure 1), i.e. the largest sub-basin of
150 the Rhine River. The main channel of the Moselle River has a length of about 545 km (Demirel
151 et al., 2013). The Moselle River basin, covering parts of the three countries France, Germany and
152 Luxembourg, has a surface area of approximately 27262 km². The three longest tributaries of the
153 Moselle River are the Saar, Sauer and Meurthe. The basin has different lithological and

154 topographic characteristics, while it has a rain dominated regime (Brenot et al., 2007). The
155 minimum, mean and maximum discharge values observed for the Moselle (at Cochem station)
156 are 14 (dry summer), 130 (long term average until 2009) and 4000 m³/s (winter), respectively
157 (Demirel et al., 2013). The mean altitude of the basin is around 340 m and the land use is
158 dominated by agriculture (54%) with arable areas, pastures and natural grasslands (Uehlinger et
159 al., 2009), and forests (37%) in the mountains and hillslopes (Demirel et al., 2019).

160



161

162

Figure 1. Moselle River network, basin boundary and elevation map

163

2.3 Data

164

165

166

167

168

Distributed hydrological models not only need hydrometeorological and geographical data as input, but also require parameters relevant for different hydrological processes such as interception and infiltration. At this point, the data availability and the spatio-temporal resolution of the input data play a vital role in the accuracy of a model. In this study, the model uses spatially distributed precipitation, temperature and potential evapotranspiration data as input

169 (Table 1). Meteorological data are from the E-OBS gridded data set on a daily basis (Haylock et
 170 al., 2008) and the discharge data at Cochem station was obtained from the Global Runoff Data
 171 Center (GRDC) in Koblenz (Germany).

172 The digital elevation model (DEM) is based on the Shuttle Radar Topography Mission
 173 (SRTM) from NASA (Ballabio et al., 2016). The soil classes are derived from the harmonized
 174 world soil database (Fischer et al., 2012), while land cover data is provided from the CORINE
 175 data set (Girard et al., 2019). Table 1 provides a brief summary of the data used in this study.

176 **Table 1** Summary of geographical and meteorological data used as input for mHM.

Variable	Description	Spatial Resolution	Temporal Resolution	Source
Q (daily)	Streamflow (Cochem station, #6336050)	Point	Daily	GRDC
P (daily)	Precipitation	24 km	Daily	E-OBS 20.0e, MODIS
ET _{ref} (daily)	Reference evapotranspiration	24 km	Daily	E-OBS 20.0°, MODIS
T _{avg} (daily)	Average air temperature	24 km	Daily	E-OBS 20.0°, MODIS
Land cover	Pervious, impervious and forest	250 m	1 map for all period	CORINE
DEM data	Slope, aspect, flow accumulation and direction	250 m	1 map for all period	SRTM
Geology class	Two main geological formations	250 m	1 map for all period	EUROPEAN SOIL DATABASE
Soil class	Soil texture data	250 m	1 map for all period	HARMONIZED WORLD SOIL DATABASE

177 (SRTM: Shuttle Radar Topography Mission, CORINE: Coordination of Information on the Environment, GRDC:
178 Global Runoff Data Center)

179 **3 Methods**

180 3.1 Meso-scale hydrological model

181 The grid-based meso-scale hydrological model (mHM) is a fully-distributed model in
182 which for each grid cell incoming and outgoing fluxes for different storage compartments are
183 calculated and the water balance of each compartment is updated after each time step (Dembélé
184 et al., 2020; Kumar et al., 2013; Samaniego et al., 2010). In mHM, runoff is transferred to the
185 downstream cells along the basin and river using three different routing methods i.e.
186 Muskingum, adaptive time step with constant celerity and adaptive time step with varying
187 celerity (Thober et al., 2019). In this study, we used adaptive time step with constant celerity
188 method as it only requires one parameter i.e. streamflow celerity. In the last decade, mHM has
189 been applied to basins in many countries in Europe (Marx et al., 2017; Samaniego et al., 2018),
190 including Germany (Baroni et al., 2019; Höllering et al., 2018; Jing et al., 2019) and Denmark
191 (Demirel et al., 2018; Koch et al., 2018), as well as to various large basins world-wide (Eisner et
192 al., 2017; Huang et al., 2018).

193 mHM is an open source software written in the Fortran 2003 language and accessible
194 from www.ufz.de/mhm, while the model is also compatible with many platforms, such as Linux,
195 Mac and Windows (Nijssen et al., 2001; Samaniego et al., 2021). One of the most appealing
196 features of the model code is the transferability between different input resolutions (Figure 2) for
197 the desired computational resolutions (mesh). The model handles different resolutions of soil
198 related data and meteorological data (Figure 2) by automatic upscaling and downscaling of high
199 resolution geographical data (L0) and coarse meteorological data (L2) to reach the user-defined

200 hydrological output resolution (L1). Also, the model provides flexibility to select a routing
 201 resolution (L11) different than the hydrological resolution (L1), so that the user can benefit from
 202 high resolution geographical input (soil, geology, aspect, LAI, elevation etc.) and does not loose
 203 time with preprocessing of meteorological data to fit the resolutions for model runs. Transferring
 204 data to a coarser resolution is done based on harmonic averaging instead of arithmetic averaging.
 205 In addition, different temporal resolutions for the model outputs can be used, e.g. daily, monthly
 206 or annual model results. For details of the process formulations, the readers and potential users
 207 may refer to the model papers (Kumar et al., 2013; Samaniego et al., 2010).

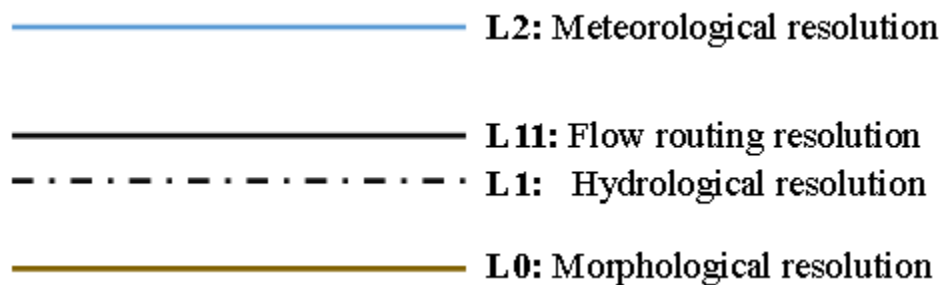


Figure 2. Model input and output scale configuration in mHM.

210 3.2 Parameter sensitivity analysis

211 Sensitivity analysis (SA) is an important step before calibration and validation of
 212 complex hydrological models to reduce the dimension of the search space. This will increase the
 213 effectiveness of the calibration process by reducing the run time. mHM includes around 55
 214 global parameters used in physically based equations representing the different hydrological
 215 processes. In this study, we applied a local sensitivity analysis method based on the Jacobian
 216 matrix available in the PEST tool (Doherty, 2010). The parameters are perturbed one-at-a-time
 217 with a particular percentage (i.e. 5%) and the change in the performance metric is observed.
 218 PEST allows one side (only increase) or two side (increase and decrease) sensitivity analysis. We

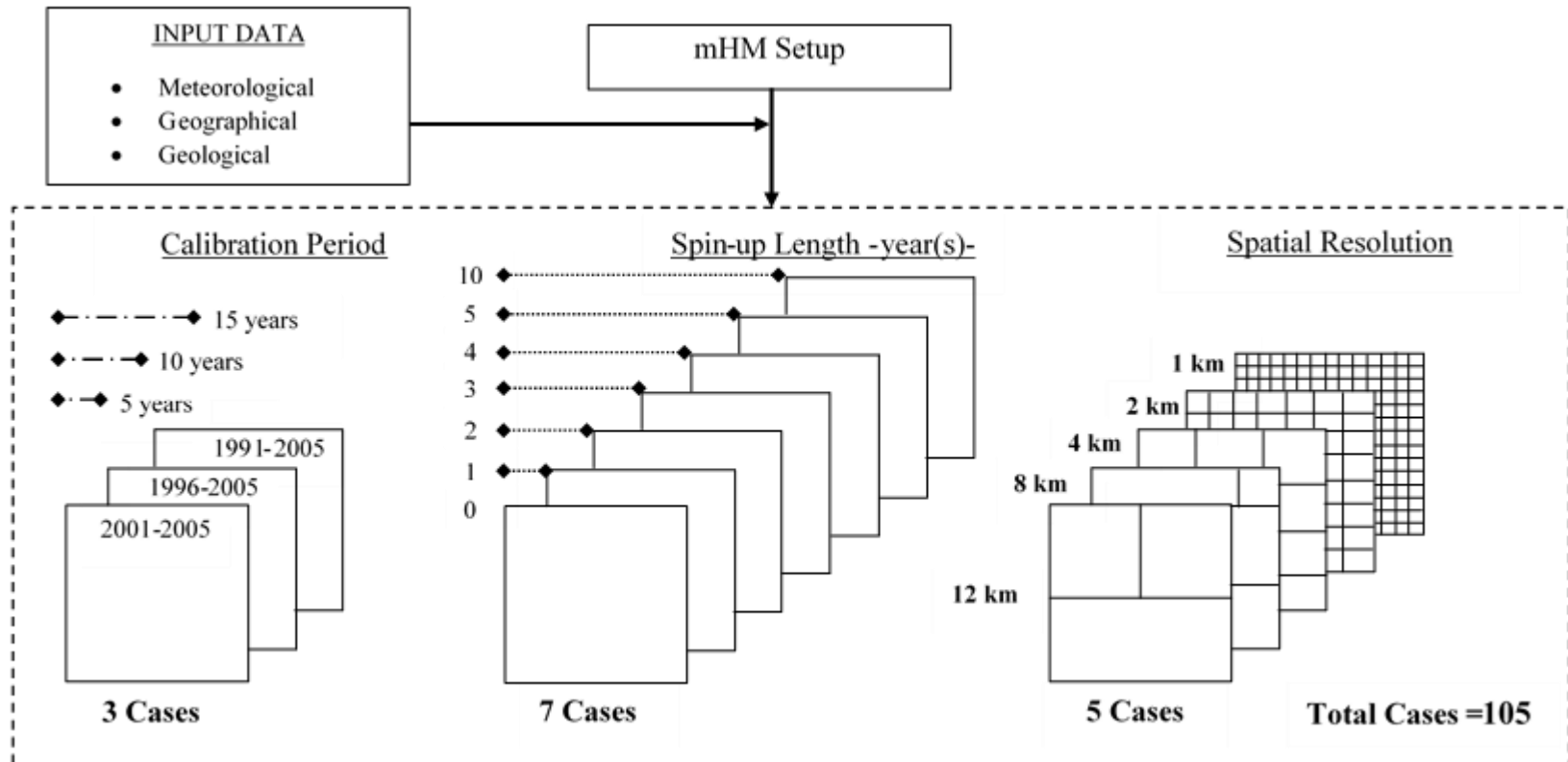
219 applied two side SA which required $2n+1$ model runs (n is the number of parameters), i.e. 55
220 parameters x 2 sides + 1 = 111 model runs.

221 3.3 Model calibration and validation

222 Since we are interested in capturing peak flows, we selected the Nash Sutcliffe Efficiency
223 (NSE), i.e. the most commonly used metric in flood hydrology (Knoben et al., 2019), to present
224 our calibration results. In this study, mHM version 5.10 was set-up for the Moselle River basin,
225 and the effects of the three factors (pillars) on the model performance were examined.
226 Accordingly, we tested all possible combinations of three factors, i.e. a total of 105 different
227 cases comprising of three calibration data lengths, seven spin-up periods and five spatial model
228 resolutions to design an appropriate calibration framework for the Moselle River basin. Here, we
229 tested spatial model resolutions varying from 1 to 12 km (Figure 3). The mHM model internally
230 upscales and downscales the input data to match the input scale to the hydrological model scale.
231 Since we identified very small effects of the routing scale on the model performance, we fixed
232 the routing scale to 6 km to save a substantial amount of run-time using the workstation
233 configuration of the AMD Ryzen Threadripper 1900X 8-Core Processor (Win-10, 4.10 GHz and
234 64GB RAM). Further, we used three different calibration periods between 1991-2005, 1996-
235 2005 and 2001-2005, corresponding to data lengths of 15, 10 and 5 years respectively. The four
236 year period between 2006 and 2009 was selected as validation period for each model since we
237 had data from 1991 to 2009. We tested seven spin-up period of 0, 1, 2, 3, 4, 5 and 10 years and
238 five different spatial model resolutions of 1, 2, 4, 8 and 12 km. It should be noted that the
239 geographical and geomorphological data of the mHM model is at a 250 m resolution and
240 meteorological inputs (P , ET_{ref} and T_{avg}) are at a 24 km resolution. The discharge data at Cochem
241 station was used both in the calibration and validation.

242 In addition, mHM internal auto-calibration tool provides four search algorithms. In this
243 study, the Dynamically Dimensioned Search (DDS) algorithm (Tolson & Shoemaker, 2007) is
244 used to calibrate the model parameters, since DDS is a fast converging method compared to local
245 gradient based methods such as the steepest descent algorithm (Huot et al., 2019). Tolson and
246 Shoemaker (2007) also highlighted that DDS outperformed one of the most popular optimization
247 algorithm in hydrology i.e. Shuffled Complex Evolutionary algorithm (Duan et al., 1992). For a
248 comprehensive analysis of the search space, we set the maximum number of iterations to 3000
249 model runs.

250



251

252

253

Figure 3. The framework of the study. Each of the 105 cases has been calibrated with the Dynamically Dimensioned Search (DDS) algorithm with a maximum number of 3000 iterations and the Nash-Sutcliffe Efficiency (NSE) as objective function.

254 **4 Results**

255 4.1 Parameter sensitivity analysis

256 Table 2 shows the most important 18 parameters using the NSE metric and sorted based
 257 on the normalized sensitivities. The normalized values are used to take into account both initial
 258 parameter values and raw sensitivity indicators from the Jacobian matrix. This is a more
 259 objective way as compared to using raw sensitivities directly, since a small change in some very
 260 small valued parameters may have a huge impact on the results whereas high valued geo-
 261 parameters may have a small raw sensitivity. In this approach, initial parameter values and raw
 262 sensitivities are multiplied (4th column) and then normalized by the maximum of this column.
 263 The normalized sensitivity value of the most sensitive parameter is 1 in this approach. Around
 264 two-third of the 55 parameters were not influential on the streamflow dynamics and similar
 265 parameters found to be sensitive in other mHM studies in different basins (Demirel et al., 2018)

266 **Table 2** Most sensitive parameters of mHM based on NSE performance.

Parameter	Initial value (-)	Raw sensitivity (-)	Abs (init. value* raw sensitivity) (-)	Normalized Sensitivity (-)
rotfrcoffore	0.9878	3.0199	2.9831	1.0000
rotfrcofclay	0.9637	1.8252	1.7590	0.5900
ptfksconst	-1.3251	0.4033	0.5344	0.1790
rotfrcofimp	0.9352	0.4676	0.4374	0.1470
ptflowconst	0.7518	0.3340	0.2511	0.0840
pet_bb	0.8942	0.2243	0.2006	0.0670
rechargecoef	6.4266	0.0260	0.1674	0.0560
pet_ap	0.4337	0.3569	0.1548	0.0520
ptfkssand	0.0094	16.2841	0.1527	0.0510
ptflowdb	-0.3323	0.4565	0.1517	0.0510
expplwintflw	0.0568	2.4514	0.1391	0.0470
pet_cc	-0.6204	0.1749	0.1085	0.0360
slwintrecks	13.3225	0.0077	0.1027	0.0340
pet_af	1.0445	0.0815	0.0851	0.0290

ptfksclay	0.0035	11.2824	0.0399	0.0130
thetanormc1	0.4722	0.0749	0.0354	0.0120
geoparam4	215.6520	0.0002	0.0335	0.0110
muskatrivslp	0.4657	0.0674	0.0314	0.0110

267

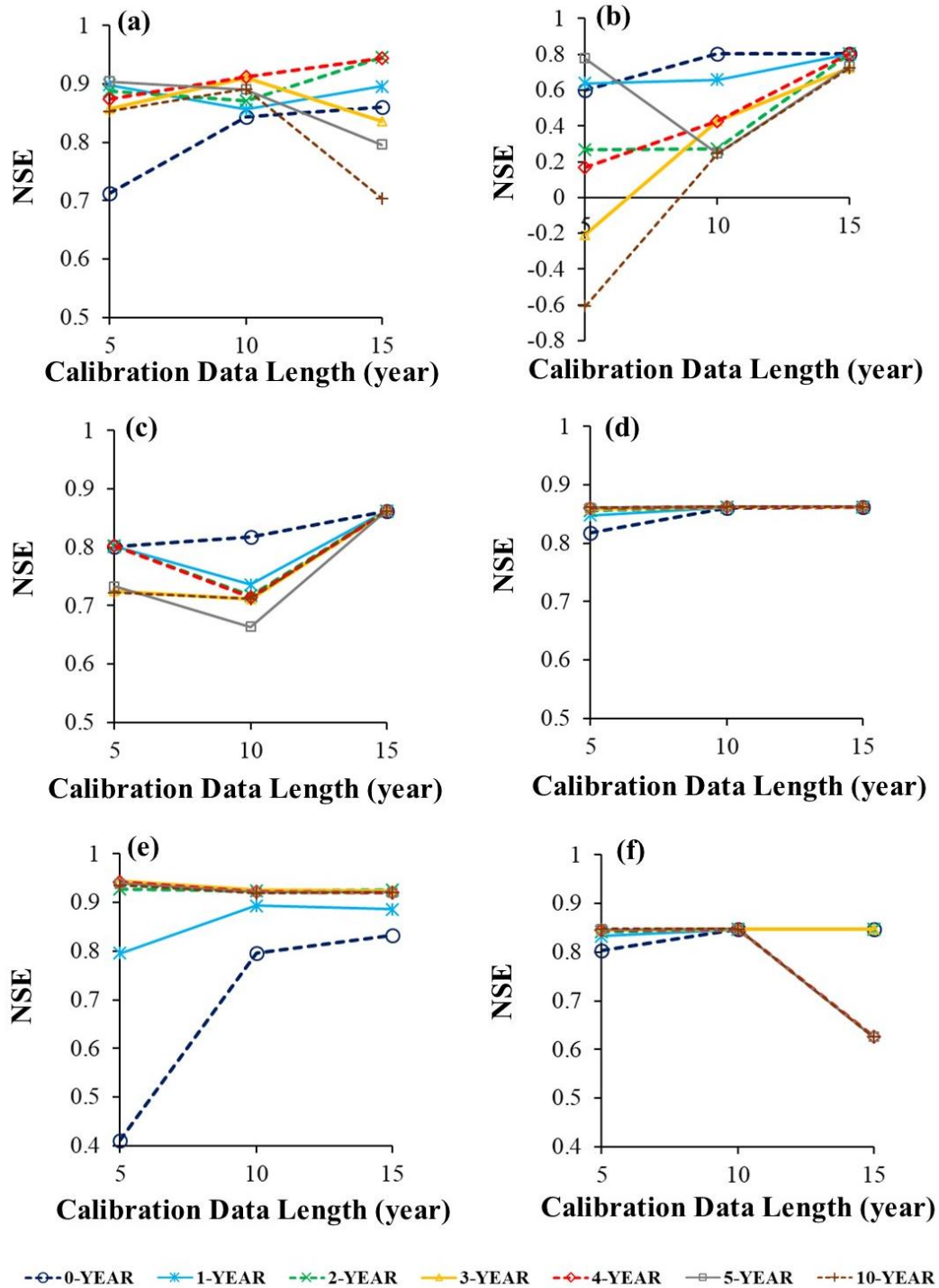
268

4.2 Effect of calibration data length on model performance

269 Figure 4 shows the model performance results in the calibration (left column) and
 270 validation (right column) periods as a function of the calibration data length for different spin-up
 271 periods and spatial resolutions. Besides the calibration results, we also present validation results
 272 as an independent test to evaluate the effects of the 105 cases.

273 For a 1 km resolution, Figure 4a shows that the model calibration performance varies
 274 depending on the spin-up period when the calibration data length increases from 5 to 15 years.
 275 Besides, Figure 4b indicates that the model validation performance increases with increasing
 276 calibration data length independently from the spin-up period. The results obtained for a 4 km
 277 resolution showed that the model calibration performance decreased when the calibration data
 278 length increased from 5 to 15 years except for a 1-year spin-up period (Figure 4c). However, the
 279 model validation performance increased when the calibration data length increased from 5 to 10
 280 years and did not show a significant change between 10 and 15 years for 4 km resolution (Figure
 281 4d). Figure 4e shows that the increase in calibration data length from 10 years to 15 years did not
 282 lead to significant changes in model calibration performance for a 8 km resolution except for a 0-
 283 year spin-up period. In addition, Figure 4f illustrates that the increase in calibration data length
 284 from 10 to 15 years deteriorates the model validation performance for spin-up periods of 4, 5 and
 285 10 years. Overall, a calibration data length of 10 years is sufficient for 4-km and 8-km
 286 resolutions, whereas setting the calibration data length to 15 years is required when the spatial
 287 resolution of the model is 1 km.

288



289

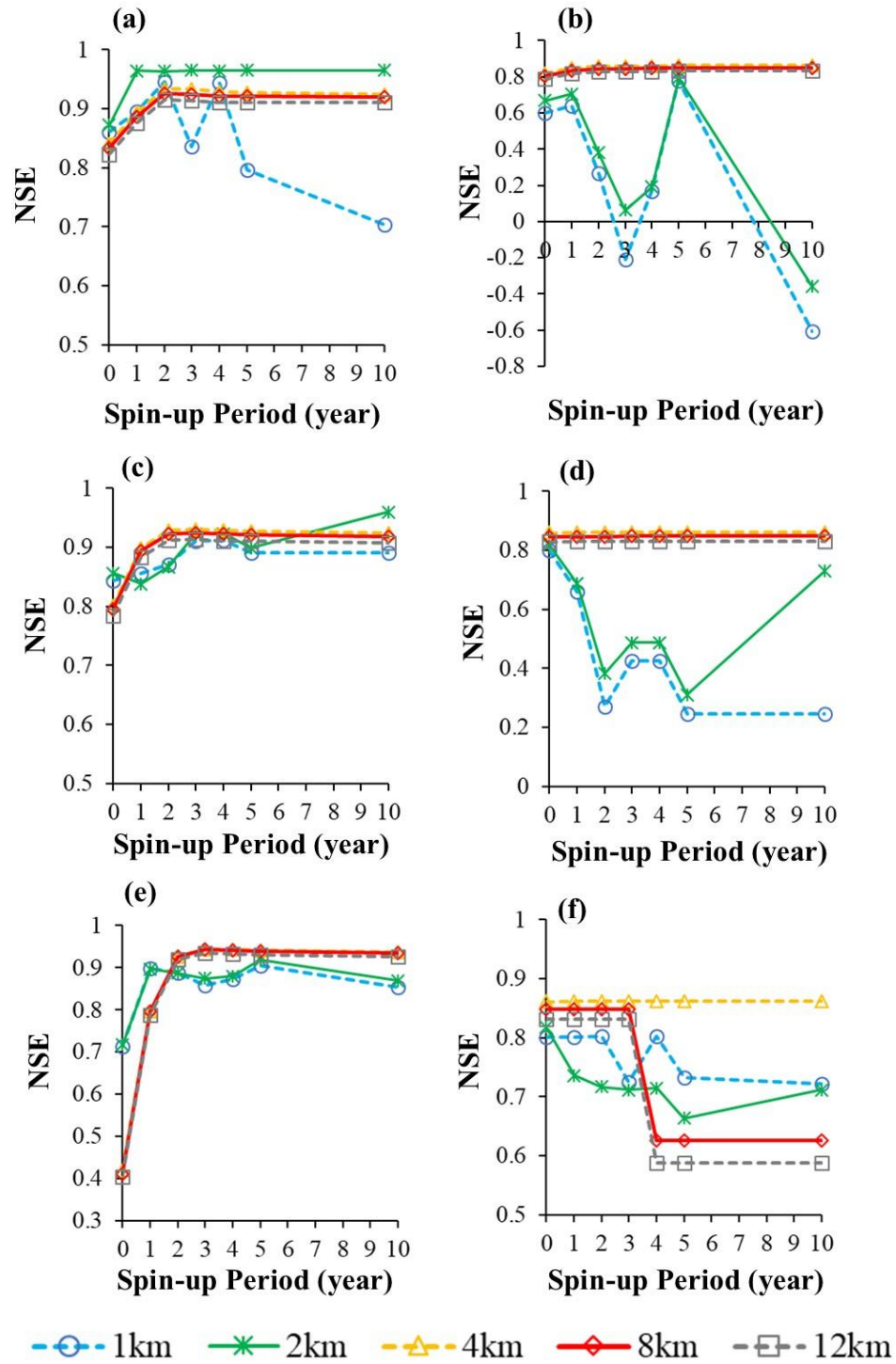
290 **Figure 4.** Model results (NSE) as a function of calibration period (length) for different spin-up
 291 periods (0 to 10 years) and different spatial resolutions; i.e. **a)** and **b)** 1 km **c)** and **d)** 4km, **e)** and

292 **f)** 8 km. Left column represents the calibration results; right column represents the validation
293 results. Horizontal axis points to three scenarios i.e. 5 year calibration covers 2001-2005, 10 year
294 calibration covers 1996-2005 and 15 year calibration covers 1991-2005.

295 4.3 Effect of spin-up period on model performance

296 Figure 5 highlights the impacts of the different spin-up periods on model performance by
297 means of the NSE for different spatial resolutions and calibration data lengths. It is apparent
298 from Figure 5 that an increase in spin-up period results in a higher model calibration
299 performance (except the case with a calibration data length of 5 years and a 1 km resolution) as
300 the model better adapts to the basin states. However, one can observe a decreasing trend in the
301 validation performance when the spin-up period was set between 0-year and 5 years, particularly
302 at a spatial resolution of 1 km and 2 km, while for a calibration data length of 15 years (Figure
303 5f), we see a similar behavior for almost each spatial resolution (except for a 4 km resolution).
304 Interestingly, for a calibration length of 15 years, from meso to coarse spatial model resolution
305 (from 4 to 12 km), the model calibration performance jumps from a NSE value of 0.4 to 0.9 as
306 the spin-up period increases from zero to two years (Figure 5e). With a few exceptions, model
307 calibration and validation results show less sensitivity to changing spin-up periods after two
308 years. On the other hand, the model calibration performance with a 1 and 2 km resolution show
309 high sensitivity to the spin-up period. This is a clear indication of the importance of selecting an
310 appropriate spin-up period for a selected spatial resolution in a systematic model calibration
311 framework. In summary, considering a calibration data length of 10 years, a spin-up period of 2
312 years is found to be adequate for the application of mHM to the Moselle River basin.

313



314

315

316

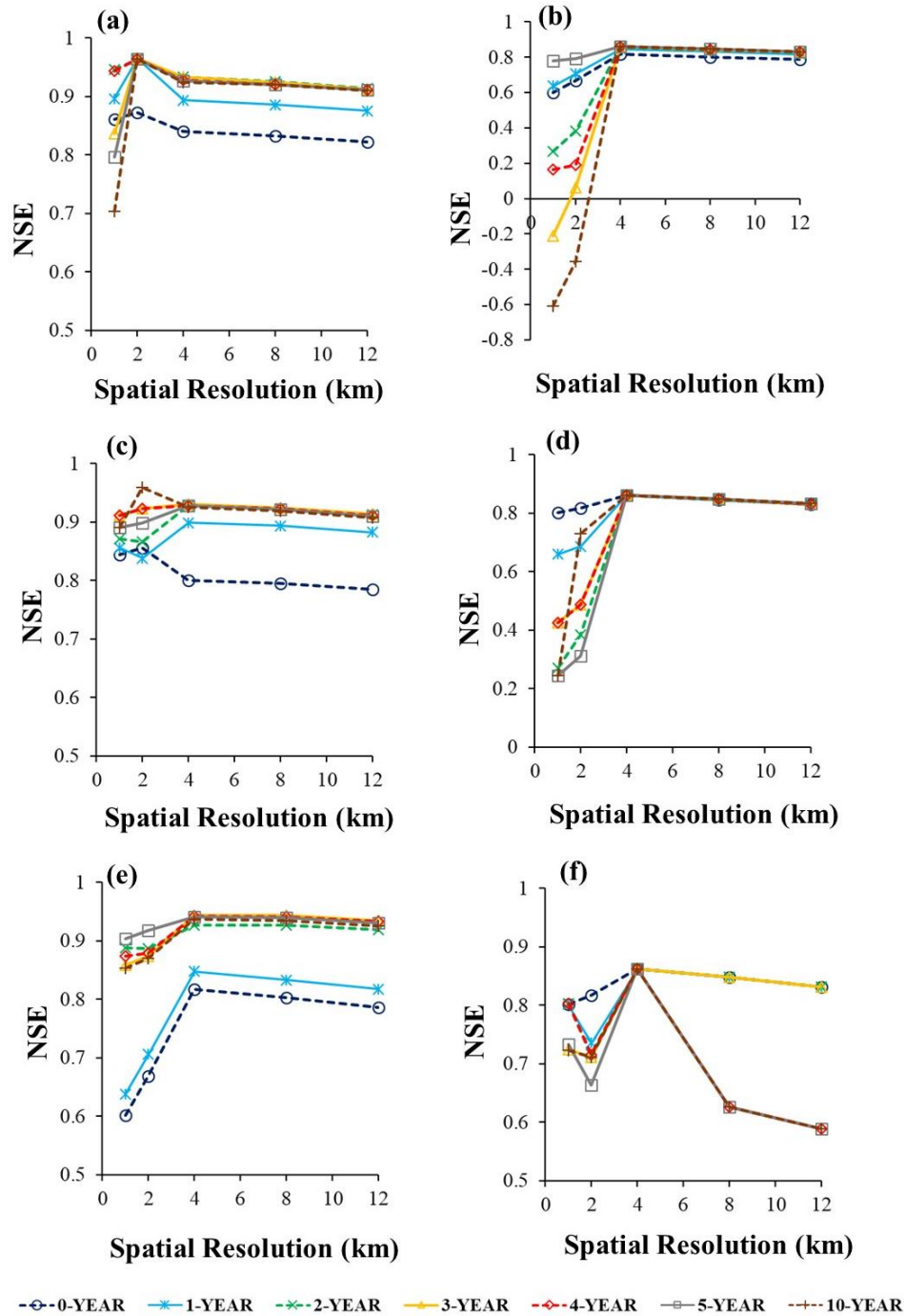
Figure 5. Model results (NSE) as a function of spin-up period for different spatial resolutions (1 km, 2km, 4km, 8km and 12 km) and calibration periods, i.e. **a)** and **b)** 5 years **c)**

317 and **d)** 10 years, **e)** and **f)** 15 years. Left column represents the calibration results; right column
318 represents the validation results.

319 4.4 Effect of spatial resolution on model performance

320 Figure 6 shows the variation in NSE in the model calibration and validation as a function
321 of spatial resolution. Colored lines represent different spin-up periods. Two adjacent sub-plots in
322 each row illustrates 5, 10 and 15 years of calibration data lengths, respectively. The results
323 obtained for both model calibration and validation illustrated that the model performance
324 increased as the model resolution increases from 1 to 4 km (except for the validation
325 performance of 15 years calibration data length). Even though this is contrary to the expectations
326 considering the physical point of view, this can be from the fact that different uncertainties in the
327 input data are less influential (reduced) after averaging data to coarser scales (upscaling). In
328 addition, Figure 6a depicts that a 2 km spatial resolution gave satisfactory results in model
329 calibration, while the model shows the best validation performance when the spatial resolution is
330 set to 4 km (Figure 6b). Also, for a calibration data length of 10 years, a 4 km resolution seems
331 the best option for both calibration and validation (Figure 6c and Figure 6d). However, some
332 inconsistencies may exist for shorter spin-up periods (such as a 0-year spin-up period). What is
333 striking about the cases with a 15-year calibration period is that there is no improvement in
334 model performance beyond a spatial resolution of 4 km (Figure 6e and Figure 6f) as the NSE
335 values tend to decrease towards 8 and 12 km resolutions.

336



337

338

339

340

341

Figure 6. Model results (NSE) as a function of spatial resolution for different spin-up periods (0 to 10 years) and calibration periods, i.e. **a)** and **b)** 5 years from 2001 to 2005 **c)** and **d)** 10 years from 1996 to 2005, **e)** and **f)** 15 years from 1991 to 2005. Left column represents the calibration results; right column represents the validation results.

342 **5 Discussion**

343 *Model calibration*

344 Model calibration is usually executed with the available data and computational
345 resources. More data and higher model resolutions are assumed to provide a more realistic
346 simulation requiring less need for model calibration than those with coarser data. In this study,
347 we analyzed 105 different model calibrations to identify an appropriate configuration of three
348 pillars, i.e. calibration data length, spin-up period and spatial resolution. We followed a smart
349 sampling approach for the choice of experimental details. For instance, instead of testing all spin-
350 up periods from one year to ten years, we only focused on zero to five years with one year
351 interval and added an experiment with a ten year spin-up period as the last case. Similarly, we
352 included only some of the most commonly used spatial model resolutions, i.e. 1, 2 and 4 km.
353 Although we could include more spatial resolutions between 250 m (L0 geographical data
354 resolution) and 24 km (L2 meteorological data resolution) such as 3, 6 and 24 km, we only
355 considered two additional resolutions (8 and 12 km). Testing 11 spin-up periods (i.e. 0 to 10
356 years) together with 10 spatial resolutions (i.e. 250 m, 500 m, 1, 2, 3, 4, 6, 8, 12 and 24 km)
357 would enormously increase the number of cases directly affecting the total duration of the
358 calibration experiments. This would also raise the question of redundancy due to the testing of
359 minor changes in the resolutions and spin-up periods. Furthermore, the model is incapable of
360 upscaling and downscaling of model inputs for the non-integer spatial resolutions, e.g. 5, 7, 9,
361 10, 11 and 23 km.

362 Although NSE is the most commonly used metric to assess hydrological model
363 performance (Mizukami et al., 2019), it is criticized for being dominated by high flow
364 performance (Pushpalatha et al., 2012). We used the DDS method, which is available in the

365 model tool, to calibrate our model. To develop a full picture of hydrological model behavior,
366 additional studies will be needed that consider multi-objective calibrations using pareto archived
367 DDS (Asadzadeh & Tolson, 2009) with additional metrics such as the Kling-Gupta Efficiency
368 (Gupta et al., 2009) and Spatial Efficiency (Demirel et al., 2018). We chose a sufficiently large
369 number of iterations (3000 runs) and reached reasonable performance results. Here, our
370 motivation was to scan a wide spectrum of the parameter domain instead of a short calibration
371 with several hundreds of iterations. Also, we only focused on single gage temporal calibration
372 with NSE. Further research should investigate effect of multi-gage and spatial model calibrations
373 using Spatial Efficiency (SPAEF) as objective function to assess the model performance
374 (Demirel et al., 2018).

375

376 *Effect of three pillars on model performance*

377 Based on the trade-off between available data and computational resources, the modeler
378 has to choose an appropriate combination of the three pillars. In this study, we assessed the effect
379 of each pillar on the model performance. It is somewhat surprising that higher spatial model
380 resolutions (1 and 2 km) lead to a higher sensitivity to the length of the calibration period. For
381 spin-up periods longer than 2 years, the model performance is relatively less sensitive. This
382 indicates that using a longer spin-up period in hydrological simulations does not always have a
383 positive effect on the model performance. From a physical point of view, the spin-up period
384 should be basin dependent and influenced by factors such as geographical heterogeneity, land
385 cover and use and flow regime. For instance, in rainfed catchments, the performance of
386 hydrological models is relatively higher than those in snowmelt dominated regions which can
387 reduce the dependency of the model for longer data length and spin-up period. However,

388 capturing rainfall heterogeneity at higher spatial resolutions is necessary for better performance.
389 The size of the catchment (Wallace et al., 2018), heterogeneity of rainfall (Nicótina et al., 2008)
390 and karstic geomorphology can greatly effect the spatio-temporal variations of hydrological
391 processes and three pillars (Zhang et al., 2020). Larger grid-size (coarser spatial resolution) can
392 be used in larger basins whereas especially for the latter cases (rainfall heterogeneity and
393 complex geology), the need for better quality data and longer time series increases significantly.
394 We are aware that spin-up periods longer than 5 years are not realistic in many hydrological
395 modeling studies (Ajami et al. 2014), however, we intended to test a wide range of periods.

396 Spatial model resolution directly effects the number of cells and the pattern of the
397 hydrological variable, e.g. actual evapotranspiration (AET), over the model domain (Booij, 2002;
398 Chen et al., 2017; Cosgrove et al., 2003; Etchevers et al., 2001; Zheng et al., 2018). For instance,
399 a single cell with spatial resolution of 24 km does not provide any pattern of AET depending on
400 the vegetation and soil type. To have a descent histogram of the spatial patterns, resolutions that
401 result in around 1000-2000 cells (pixels) are required to calculate spatial performance as shown
402 in other basins (Demirel et al., 2018).

403

404 *Uncertainties and Data*

405 Assessing uncertainties raising from model structure, inputs and parameters is important for
406 assessing the reliability of the results. Model structure uncertainty can be analyzed by using
407 multiple models (Demirel et al., 2013). Here, we only focused on one distributed model (i.e.
408 mHM) and the EOBS meteorological dataset. Parameter uncertainty is assumed to be reduced
409 during the model calibration. There are still many unanswered questions about the model input
410 uncertainty. To compare the effect of input uncertainty on the results, the ERA5 meteorological

411 dataset (Hersbach et al., 2020) can be used in the model in addition to the EOBS dataset (Cornes
412 et al., 2018). Further, we chose aspect based potential ET correction in the model as leaf area
413 index (LAI) based potential ET correction will be a topic of our future study. It is assumed that
414 the LAI based potential ET correction would yield better AET estimates; therefore, better
415 discharge performance as compared to those with aspect data (Demirel et al., 2018).

416 Data quality and length can be big issues for modelers from developing countries. Even
417 though the modeler has a long time series with unlimited computational resources, a ten-year
418 part of the new data set with a spin-up period of two or three years is sufficient for the model
419 calibration. Then, the remaining, i.e. not wasted, data can be used for model validation (Royer-
420 Gaspard et al., 2021). Further work should examine the effect of model input data resolution in
421 addition to the model spatial resolution. Also, the length of the validation period can be varied in
422 addition to the length of the calibration period.

423

424 **6 Conclusions**

425 This study was designed to comprehensively investigate the effects of three user-defined
426 model configurations that are usually determined based on local expert knowledge and available
427 data. We focused on the identification of the appropriate length of the calibration period, the
428 length of the spin-up period and the appropriate spatial model resolution for the Moselle River
429 basin. For that, we used a fully distributed hydrological model (mHM) and performed 105
430 different calibrations with the DDS optimization algorithm and NSE objective function. The 105
431 cases are combinations of three calibration periods, seven spin-up periods and five spatial model
432 resolutions.

433 The main conclusions from this work can be summarized as follows:

434 • Based on the results of the comparison of three calibration data lengths, 10 years
435 is found to be an appropriate length for the Moselle River basin. The interaction between
436 calibration period and 1-2 km spatial resolution has the strongest effect on the results.

437 • Based on the results of the comparison of three spin-up periods, two years of spin-
438 up period in addition to the 10 years of calibration data is found to be sufficient for the model to
439 adopt to the initial conditions in the Moselle River basin. Longer spin-up periods than two years
440 did not significantly improve the model calibration and validation performances.

441 • Based on the results of the comparison of five spatial resolutions, 4 km is found to
442 be the most appropriate model resolution for the Moselle River basin since the performance
443 slightly deteriorated at coarser resolutions (i.e. 8 and 12 km).

444 Overall, the three factors analyzed in our study are usually overlooked in hydrological
445 modeling. However, the results showed that we should carefully analyze the different

446 combinations of calibration data length, spin-up period and spatial resolution instead of selecting
447 an arbitrary combination. It is important to mention that our multi-case analysis framework
448 proposed in this study can be applied to any other spatially distributed model and catchment.

449

450 **Acknowledgments, Samples, and Data**

451 We acknowledge the financial support for the SPACE project by the Villum Foundation
452 (<http://villumfonden.dk/>) through their Young Investigator Programme (grant VKR023443). The
453 second author (MCD) is supported by the National Center for High Performance Computing of
454 Turkey (UHeM) under grant number 1007292019 and Ir. Cornelis Lely Stichting (grant
455 20957310). The mHM v5.10 model (available at <https://git.ufz.de/mhm>) together with all the set-
456 up data was provided by UFZ in Leipzig, Germany.

457 **References**

- 458 Abdo, K. S., Fiseha, B. M., Rientjes, T. H. M., Gieske, A. S. M., & Haile, A. T. (2009). Assessment of climate
459 change impacts on the hydrology of Gilgel Abay catchment in Lake Tana Basin, Ethiopia. *Hydrological
460 Processes*, 2274(November 2008), n/a-n/a. <https://doi.org/10.1002/hyp.7363>
- 461 Ajami, H., Evans, J. P., McCabe, M. F., & Stisen, S. (2014). Technical Note: Reducing the spin-up time of
462 integrated surface water–groundwater models. *Hydrology and Earth System Sciences*, 18(12), 5169–5179.
463 <https://doi.org/10.5194/hess-18-5169-2014>
- 464 Ajami, Hoori, McCabe, M. F., Evans, J. P., & Stisen, S. (2014). Assessing the impact of model spin-up on surface
465 water-groundwater interactions using an integrated hydrologic model. *Water Resources Research*, 50(3),
466 2636–2656. <https://doi.org/10.1002/2013WR014258>
- 467 Andersen, J., Refsgaard, J. C., & Jensen, K. H. (2001). Distributed hydrological modelling of the Senegal River
468 Basin - Model construction and validation. *Journal of Hydrology*, 247(3–4), 200–214.
469 [https://doi.org/10.1016/S0022-1694\(01\)00384-5](https://doi.org/10.1016/S0022-1694(01)00384-5)
- 470 Asadzadeh, M., & Tolson, B. A. (2009). A new multi-objective algorithm, pareto archived DDS. In *Proceedings of
471 the 11th annual conference companion on Genetic and evolutionary computation conference - GECCO '09* (p.
472 1963). New York, New York, USA: ACM Press. <https://doi.org/10.1145/1570256.1570259>
- 473 Ashraf, A. (2013). Changing Hydrology of the Himalayan Watershed. In *Current Perspectives in Contaminant
474 Hydrology and Water Resources Sustainability* (Vol. i, p. 13). InTech. <https://doi.org/10.5772/54492>
- 475 Ballabio, C., Panagos, P., & Monatanarella, L. (2016). Mapping topsoil physical properties at European scale using
476 the LUCAS database. *Geoderma*, 261, 110–123. <https://doi.org/10.1016/j.geoderma.2015.07.006>
- 477 Baroni, G., Schalge, B., Rakovec, O., Kumar, R., Schüler, L., Samaniego, L., et al. (2019). A Comprehensive
478 Distributed Hydrological Modeling Intercomparison to Support Process Representation and Data Collection
479 Strategies. *Water Resources Research*, 990–1010. <https://doi.org/10.1029/2018WR023941>
- 480 Beck, H. E., Vergopolan, N., Pan, M., Levizzani, V., van Dijk, A. I. J. M., Weedon, G. P., et al. (2017). Global-scale
481 evaluation of 22 precipitation datasets using gauge observations and hydrological modeling. *Hydrology and
482 Earth System Sciences*, 21(12), 6201–6217. <https://doi.org/10.5194/hess-21-6201-2017>
- 483 Blöschl, G., & Sivapalan, M. (1995). Scale issues in hydrological modelling: A review. *Hydrological Processes*,
484 9(3–4), 251–290. Retrieved from <http://dx.doi.org/10.1002/hyp.3360090305>

- 485 Booij, M. J. (2002). Modelling the effects of spatial and temporal resolution of rainfall and basin model on extreme
486 river discharge. *Hydrological Sciences Journal*, 47(2), 307–320. <https://doi.org/10.1080/02626660209492932>
- 487 Booij, M. J. (2005). Impact of climate change on river flooding assessed with different spatial model resolutions.
488 *Journal of Hydrology*, 303(1–4), 176–198. <https://doi.org/10.1016/j.jhydrol.2004.07.013>
- 489 Brenot, A., Carignan, J., France-Lanord, C., & Benoît, M. (2007). Geological and land use control on $\delta^{34}\text{S}$ and
490 $\delta^{18}\text{O}$ of river dissolved sulfate: The Moselle river basin, France. *Chemical Geology*, 244(1–2), 25–41.
491 <https://doi.org/10.1016/j.chemgeo.2007.06.003>
- 492 Bucchignani, E., Mercogliano, P., Rianna, G., & Panitz, H.-J. (2016). Analysis of ERA-Interim-driven COSMO-
493 CLM simulations over Middle East - North Africa domain at different spatial resolutions. *International*
494 *Journal of Climatology*, 36(9), 3346–3369. <https://doi.org/10.1002/joc.4559>
- 495 Chen, Y., Li, J., Wang, H., Qin, J., & Dong, L. (2017). Large-watershed flood forecasting with high-resolution
496 distributed hydrological model. *Hydrology and Earth System Sciences*, 21(2), 735–749.
497 <https://doi.org/10.5194/hess-21-735-2017>
- 498 Cornes, R. C., van der Schrier, G., van den Besselaar, E. J. M., & Jones, P. D. (2018). An Ensemble Version of the
499 E-OBS Temperature and Precipitation Data Sets. *Journal of Geophysical Research: Atmospheres*, 123(17),
500 9391–9409. <https://doi.org/10.1029/2017JD028200>
- 501 Cosgrove, B. A., Lohmann, D., Mitchell, K. E., Houser, P. R., Wood, E. F., Schaake, J. C., et al. (2003). Land
502 surface model spin-up behavior in the North American Land Data Assimilation System (NLDAS). *Journal of*
503 *Geophysical Research D: Atmospheres*, 108(22). <https://doi.org/10.1029/2002jd003316>
- 504 Cuo, L., Giambelluca, T. W., Ziegler, A. D., & Nullet, M. A. (2006). Use of the distributed hydrology soil
505 vegetation model to study road effects on hydrological processes in Pang Khum Experimental Watershed,
506 northern Thailand. *Forest Ecology and Management*, 224(1–2), 81–94.
507 <https://doi.org/10.1016/j.foreco.2005.12.009>
- 508 Daggupati, P., Pai, N., Ale, S., Douglas-Mankin, K. R., Zeckoski, R. W., Jeong, J., et al. (2015). A recommended
509 calibration and validation strategy for hydrologic and water quality models. *Transactions of the ASABE*, 58(6),
510 1705–1719. <https://doi.org/10.13031/trans.58.10712>
- 511 Dehotin, J., & Braud, I. (2008). Which spatial discretization for distributed hydrological models? Proposition of a
512 methodology and illustration for medium to large-scale catchments. *Hydrology and Earth System Sciences*,

- 513 12(3), 769–796. <https://doi.org/10.5194/hess-12-769-2008>
- 514 Dembélé, M., Hrachowitz, M., Savenije, H. H. G., Mariéthoz, G., & Schaefli, B. (2020). Improving the Predictive
515 Skill of a Distributed Hydrological Model by Calibration on Spatial Patterns With Multiple Satellite Data Sets.
516 *Water Resources Research*, 56(1). <https://doi.org/10.1029/2019WR026085>
- 517 Demirel, Özen, Orta, Toker, Demir, Ekmekcioğlu, et al. (2019). Additional Value of Using Satellite-Based Soil
518 Moisture and Two Sources of Groundwater Data for Hydrological Model Calibration. *Water*, 11(10), 2083.
519 <https://doi.org/10.3390/w11102083>
- 520 Demirel, M. C., Booij, M. J., & Hoekstra, A. Y. (2013). Effect of different uncertainty sources on the skill of 10 day
521 ensemble low flow forecasts for two hydrological models. *Water Resources Research*, 49(7), 4035–4053.
522 <https://doi.org/10.1002/wrcr.20294>
- 523 Demirel, M. C., Mai, J., Mendiguren, G., Koch, J., Samaniego, L., & Stisen, S. (2018). Combining satellite data and
524 appropriate objective functions for improved spatial pattern performance of a distributed hydrologic model.
525 *Hydrol. Earth Syst. Sci.*, 22(2), 1299–1315. <https://doi.org/10.5194/hess-22-1299-2018>
- 526 Doherty, J. (2010). *PEST: Model-Independent Parameter Estimation, User Manual: 5th Edition. PEST Manual.*
- 527 Duan, Q. Q.-Y. Y., Sorooshian, S., & Gupta, V. Effective and efficient global optimization for conceptual rainfall-
528 runoff models, 28 *Water Resources Research* § (1992). <https://doi.org/10.1029/91WR02985>
- 529 Eisner, S., Flörke, M., Chamorro, A., Daggupati, P., Donnelly, C., Huang, J., et al. (2017). An ensemble analysis of
530 climate change impacts on streamflow seasonality across 11 large river basins. *Climatic Change*, 141(3), 401–
531 417. <https://doi.org/10.1007/s10584-016-1844-5>
- 532 Epstein, D. J., Welles, E., & Day, G. N. (1998). Probabilistic Hydrologic Forecasting Methods and Tools. In
533 *Proceedings of the First Federal Interagency Hydrologic Modeling Conference* (pp. 6(17-24)). Las Vegas,
534 Nevada: Subcommittee on Hydrology of the Interagency Advisory Committee on Water Data.
- 535 Etchevers, P., Durand, Y., Habets, F., Martin, E., & Noilhan, J. (2001). Impact of spatial resolution on the
536 hydrological simulation of the Durance high-Alpine catchment, France. *Annals of Glaciology*, 32, 87–92.
537 <https://doi.org/10.3189/172756401781819337>
- 538 Fischer, G., Nachtergaele, F., Prieler, S., Velthuisen, H. T. van, Verelst, L., & Wiberg, D. (2012). *Global Agro-
539 ecological Zones–Model Documentation (GAEZ v. 3.0). Food and Agriculture Organization of the United
540 Nations.*

- 541 Gelleszun, M., Kreye, P., & Meon, G. (2017). Representative parameter estimation for hydrological models using a
542 lexicographic calibration strategy. *Journal of Hydrology*, 553, 722–734.
543 <https://doi.org/10.1016/j.jhydrol.2017.08.015>
- 544 Girard, M.-C., Girard, C., Courault, D., Gilliot, J.-M., Loubersac, L., Meyer-Roux, J., et al. (2019). Corine Land
545 Cover. In *Processing of Remote Sensing Data*. <https://doi.org/10.1201/9780203741917-19>
- 546 Gires, A., Giangola-Murzyn, A., Abbes, J. B., Tchiguirinskaia, I., Schertzer, D., & Lovejoy, S. (2015). Impacts of
547 small scale rainfall variability in urban areas: a case study with 1D and 1D/2D hydrological models in a
548 multifractal framework. *Urban Water Journal*, 12(8), 607–617.
549 <https://doi.org/10.1080/1573062X.2014.923917>
- 550 Gupta, H. V., Kling, H., Yilmaz, K. K., & Martinez, G. F. (2009). Decomposition of the mean squared error and
551 NSE performance criteria: Implications for improving hydrological modelling. *Journal of Hydrology*, 377(1–
552 2), 80–91. <https://doi.org/10.1016/j.jhydrol.2009.08.003>
- 553 Haylock, M. R., Hofstra, N., Klein Tank, A. M. G., Klok, E. J., Jones, P. D., & New, M. (2008). A European daily
554 high-resolution gridded data set of surface temperature and precipitation for 1950–2006. *Journal of*
555 *Geophysical Research Atmospheres*, 113(20). <https://doi.org/10.1029/2008JD010201>
- 556 Herman, M. R., Nejadhashemi, A. P., Abouali, M., Hernandez-Suarez, J. S., Daneshvar, F., Zhang, Z., et al. (2018).
557 Evaluating the role of evapotranspiration remote sensing data in improving hydrological modeling
558 predictability. *Journal of Hydrology*, 556(1), 39–49. <https://doi.org/10.1016/j.jhydrol.2017.11.009>
- 559 Hersbach, H., Bell, B., Berrisford, P., Hirahara, S., Horányi, A., Muñoz-Sabater, J., et al. (2020). The ERA5 global
560 reanalysis. *Quarterly Journal of the Royal Meteorological Society*, 146(730), 1999–2049.
561 <https://doi.org/10.1002/qj.3803>
- 562 Höllering, S., Wienhöfer, J., Ihringer, J., Samaniego, L., & Zehe, E. (2018). Regional analysis of parameter
563 sensitivity for simulation of streamflow and hydrological fingerprints. *Hydrology and Earth System Sciences*,
564 22(1), 203–220. <https://doi.org/10.5194/hess-22-203-2018>
- 565 Huang, S., Kumar, R., Rakovec, O., Aich, V., Wang, X., Samaniego, L., et al. (2018). Multimodel assessment of
566 flood characteristics in four large river basins at global warming of 1.5, 2.0 and 3.0 K above the pre-industrial
567 level. *Environmental Research Letters*, 13(12). <https://doi.org/10.1088/1748-9326/aae94b>
- 568 Huot, P. L., Poulin, A., Audet, C., & Alarie, S. (2019). A hybrid optimization approach for efficient calibration of

- 569 computationally intensive hydrological models. *Hydrological Sciences Journal*, 64(10), 1204–1222.
570 <https://doi.org/10.1080/02626667.2019.1624922>
- 571 Jing, M., Heße, F., Kumar, R., Kolditz, O., Kalbacher, T., & Attinger, S. (2019). Influence of input and parameter
572 uncertainty on the prediction of catchment-scale groundwater travel time distributions. *Hydrology and Earth
573 System Sciences*, 23(1), 171–190. <https://doi.org/10.5194/hess-23-171-2019>
- 574 Kim, K. B., Kwon, H. H., & Han, D. (2018). Exploration of warm-up period in conceptual hydrological modelling.
575 *Journal of Hydrology*, 556, 194–210. <https://doi.org/10.1016/j.jhydrol.2017.11.015>
- 576 Knoben, W. J. M., Freer, J. E., & Woods, R. A. (2019). Technical note: Inherent benchmark or not? Comparing
577 Nash–Sutcliffe and Kling–Gupta efficiency scores. *Hydrology and Earth System Sciences*, 23(10), 4323–4331.
578 <https://doi.org/10.5194/hess-23-4323-2019>
- 579 Koch, J., Demirel, M. C., & Stisen, S. (2018). The SPAtial EFFiciency metric (SPAEF): multiple-component
580 evaluation of spatial patterns for optimization of hydrological models. *Geoscientific Model Development*,
581 11(5), 1873–1886. <https://doi.org/10.5194/gmd-11-1873-2018>
- 582 Koren, V. I., Finnerty, B. D., Schaake, J. C., Smith, M. B., Seo, D. J., & Duan, Q. Y. (1999). Scale dependencies of
583 hydrologic models to spatial variability of precipitation. *Journal of Hydrology*, 217(3–4), 285–302.
584 [https://doi.org/10.1016/S0022-1694\(98\)00231-5](https://doi.org/10.1016/S0022-1694(98)00231-5)
- 585 Kumar, R., Samaniego, L., & Attinger, S. (2013). Implications of distributed hydrologic model parameterization on
586 water fluxes at multiple scales and locations. *Water Resources Research*, 49(1), 360–379.
587 <https://doi.org/10.1029/2012WR012195>
- 588 Lohmann, D., Raschke, E., Nijssen, B., & Lettenmaier, D. P. (1998). Hydrologie à l'échelle régionale: II.
589 Application du modèle VIC-2L sur la rivière Weser, Allemagne. *Hydrological Sciences Journal*, 43(1), 143–
590 158. <https://doi.org/10.1080/02626669809492108>
- 591 Madsen, H. (2003). Parameter estimation in distributed hydrological catchment modelling using automatic
592 calibration with multiple objectives. *Advances in Water Resources*, 26(2), 205–216.
593 [https://doi.org/10.1016/S0309-1708\(02\)00092-1](https://doi.org/10.1016/S0309-1708(02)00092-1)
- 594 Marx, A., Kumar, R., Thober, S., Zink, M., Wanders, N., Wood, E. F., et al. (2017). Climate change alters low flows
595 in Europe under a 1.5, 2, and 3 degree global warming. *Hydrology and Earth System Sciences Discussions*, 1–
596 24. <https://doi.org/10.5194/hess-2017-485>

- 597 Merz, R., Parajka, J., & Blöschl, G. (2009). Scale effects in conceptual hydrological modeling. *Water Resources*
598 *Research*, 45(9), W09405. <https://doi.org/10.1029/2009wr007872>
- 599 Mizukami, N., Rakovec, O., Newman, A. J., Clark, M. P., Wood, A. W., Gupta, H. V., & Kumar, R. (2019). On the
600 choice of calibration metrics for “high-flow” estimation using hydrologic models. *Hydrology and Earth*
601 *System Sciences*, 23(6), 2601–2614. <https://doi.org/10.5194/hess-23-2601-2019>
- 602 Näschen, K., Diekkrüger, B., Leemhuis, C., Steinbach, S., Seregina, L., Thonfeld, F., & van der Linden, R. (2018).
603 Hydrological Modeling in Data-Scarce Catchments: The Kilombero Floodplain in Tanzania. *Water*, 10(5),
604 599. <https://doi.org/10.3390/w10050599>
- 605 Nicótina, L., Alessi Celegon, E., Rinaldo, A., & Marani, M. (2008). On the impact of rainfall patterns on the
606 hydrologic response. *Water Resources Research*, 44(12). <https://doi.org/10.1029/2007WR006654>
- 607 Nijssen, B., O’Donnell, G. M., Lettenmaier, D. P., Lohmann, D., & Wood, E. F. (2001). Predicting the discharge of
608 global rivers. *Journal of Climate*, 14(15), 3307–3323.
- 609 Pang, J., Zhang, H., Xu, Q., Wang, Y., Wang, Y., Zhang, O., & Hao, J. (2020). Hydrological evaluation of open-
610 access precipitation data using SWAT at multiple temporal and spatial scales. *Hydrology and Earth System*
611 *Sciences*, 24(7), 3603–3626. <https://doi.org/10.5194/hess-24-3603-2020>
- 612 Perrin, C., Oudin, L., Andreassian, V., Rojas-Serna, C., Michel, C., & Mathevet, T. (2007). Impact of limited
613 streamflow data on the efficiency and the parameters of rainfall—runoff models. *Hydrological Sciences*
614 *Journal*, 52(1), 131–151. <https://doi.org/10.1623/hysj.52.1.131>
- 615 Pushpalatha, R., Perrin, C., Moine, N. Le, & Andréassian, V. (2012). A review of efficiency criteria suitable for
616 evaluating low-flow simulations. *Journal of Hydrology*, 420–421, 171–182.
617 <https://doi.org/10.1016/j.jhydrol.2011.11.055>
- 618 Rahman, M. M., Lu, M., & Kyi, K. H. (2016). Seasonality of hydrological model spin-up time: a case study using
619 the Xinanjiang model. *Hydrology and Earth System Sciences Discussions*, 1–22. [https://doi.org/10.5194/hess-](https://doi.org/10.5194/hess-2016-316)
620 2016-316
- 621 Raihan, F., Beaumont, L. J., Maina, J., Saiful Islam, A., & Harrison, S. P. (2020). Simulating streamflow in the
622 Upper Halda Basin of southeastern Bangladesh using SWAT model. *Hydrological Sciences Journal*, 65(1),
623 138–151. <https://doi.org/10.1080/02626667.2019.1682149>
- 624 Revilla-Romero, B., Wanders, N., Burek, P., Salamon, P., & de Roo, A. (2016). Integrating remotely sensed surface

- 625 water extent into continental scale hydrology. *Journal of Hydrology*, 543, 659–670.
626 <https://doi.org/10.1016/j.jhydrol.2016.10.041>
- 627 Rodell, M., Houser, P. R., Berg, A. A., & Famiglietti, J. S. (2005). Evaluation of 10 methods for initializing a land
628 surface model. *Journal of Hydrometeorology*, 6(2), 146–155. <https://doi.org/10.1175/JHM414.1>
- 629 Royer-Gaspard, P., Andréassian, V., & Guillaume, T. (2021). Technical note: PMR – a proxy metric to assess
630 hydrological model robustness in a changing climate. *Hydrol. Earth Syst. Sci. Discuss., preprint*.
631 <https://doi.org/10.5194/hess-2021-58>
- 632 Samaniego, Brenner, J., Craven, J., Cuntz, M., Dalmaso, G., Demirel, M. C., et al. (2021, February 3). mesoscale
633 Hydrologic Model - mHM v5.11.0. Leipzig. <https://doi.org/10.5281/ZENODO.4462822>
- 634 Samaniego, L., Thober, S., Kumar, R., Wanders, N., Rakovec, O., Pan, M., et al. (2018). Anthropogenic warming
635 exacerbates European soil moisture droughts. *Nature Climate Change*, 8(5), 421–426.
636 <https://doi.org/10.1038/s41558-018-0138-5>
- 637 Samaniego, Luis, Kumar, R., & Attinger, S. (2010). Multiscale parameter regionalization of a grid-based hydrologic
638 model at the mesoscale. *Water Resources Research*, 46(5), W05523. <https://doi.org/10.1029/2008WR007327>
- 639 Shi, X., Wood, A. W., & Lettenmaier, D. P. (2008). How essential is hydrologic model calibration to seasonal stream
640 flow forecasting? *Journal of Hydrometeorology*, 9(6), 1350–1363. <https://doi.org/10.1175/2008JHM1001.1>
- 641 Shrestha, R., & Houser, P. (2010). A heterogeneous land surface model initialization study. *Journal of Geophysical*
642 *Research Atmospheres*, 115(19), 1–10. <https://doi.org/10.1029/2009JD013252>
- 643 Simunek, J. J., Genuchten, M. T. Van, & Šejna, M. (2012). HYDRUS: Model Use, Calibration, and Validation.
644 *Transactions of the ASABE*, 55(4), 1263–1276. <https://doi.org/10.13031/2013.42239>
- 645 Sood, A., & Smakhtin, V. (2015). Revue des modèles hydrologiques globaux. *Hydrological Sciences Journal*, 60(4),
646 549–565. <https://doi.org/10.1080/02626667.2014.950580>
- 647 Sood, A., Muthuwatta, L., & McCartney, M. (2013). A SWAT evaluation of the effect of climate change on the
648 hydrology of the Volta River basin. *Water International*, 38(3), 297–311.
649 <https://doi.org/10.1080/02508060.2013.792404>
- 650 Sorooshian, S., Gupta, H. V., & Rodda, J. C. (1997). *Land Surface Processes in Hydrology: Trials and Tribulations*
651 *of Modeling and Measuring*. (S. Sorooshian, H. V. Gupta, & J. C. Rodda, Eds.). Berlin, Heidelberg: Springer
652 Berlin Heidelberg. <https://doi.org/10.1007/978-3-642-60567-3>

- 653 Sreedevi, S., & Eldho, T. I. (2019). A two-stage sensitivity analysis for parameter identification and calibration of a
654 physically-based distributed model in a river basin. *Hydrological Sciences Journal*, 64(6), 701–719.
655 <https://doi.org/10.1080/02626667.2019.1602730>
- 656 Thober, S., Cuntz, M., Kelbling, M., Kumar, R., Mai, J., & Samaniego, L. (2019). The multiscale routing model
657 mRM v1.0: simple river routing at resolutions from 1 to 50 km. *Geoscientific Model Development*, 12(6),
658 2501–2521. <https://doi.org/10.5194/gmd-12-2501-2019>
- 659 Tian, J., Liu, J., Wang, Y., Wang, W., Li, C., & Hu, C. (2020). A coupled atmospheric-hydrologic modeling system
660 with variable grid sizes for rainfall-runoff simulation in semi-humid and semi-arid watersheds: How does the
661 coupling scale affects the results? *Hydrology and Earth System Sciences Discussions*, 1–36.
662 <https://doi.org/10.5194/hess-2019-587>
- 663 Tolson, B. A., & Shoemaker, C. A. (2007). Dynamically dimensioned search algorithm for computationally efficient
664 watershed model calibration. *Water Resources Research*, 43(1). <https://doi.org/10.1029/2005WR004723>
- 665 Uehlinger, U., Wantzen, K. M., Leuven, R. S. E. W., & Arndt, H. (2009). The Rhine River Basin. In *Rivers of*
666 *Europe* (pp. 199–245). London: Academic Press. Retrieved from
667 <http://www.sciencedirect.com/science/article/B8M9H-4VJ0XHB-R/2/5a2ee83572d773dd7ec4e308c6a3c292>
- 668 Wallace, C., Flanagan, D., & Engel, B. (2018). Evaluating the Effects of Watershed Size on SWAT Calibration.
669 *Water*, 10(7), 898. <https://doi.org/10.3390/w10070898>
- 670 Westerberg, I. K., Sikorska-Senoner, A. E., Viviroli, D., Vis, M., & Seibert, J. (2020). Hydrological model
671 calibration with uncertain discharge data. *Hydrological Sciences Journal*, 00(00), 1–16.
672 <https://doi.org/10.1080/02626667.2020.1735638>
- 673 Xu, Y. P., Zhang, X., Ran, Q., & Tian, Y. (2013). Impact of climate change on hydrology of upper reaches of
674 Qiantang River Basin, East China. *Journal of Hydrology*, 483, 51–60.
675 <https://doi.org/10.1016/j.jhydrol.2013.01.004>
- 676 Yang, Z. L., Dickinson, R. E., Henderson-Selles, A., & Pitman, A. J. (1995). Preliminary study of spin-up processes
677 in land surface models with the first stage data of project for intercomparison of land surface parameterization
678 schemes phase 1(a). *Journal of Geophysical Research*, 100(D8). <https://doi.org/10.1029/95jd01076>
- 679 Zhang, Z., Chen, X., Cheng, Q., Li, S., Yue, F., Peng, T., et al. (2020). Coupled hydrological and biogeochemical
680 modelling of nitrogen transport in the karst critical zone. *Science of The Total Environment*, 732, 138902.

681 <https://doi.org/10.1016/j.scitotenv.2020.138902>

682 Zheng, F., Maier, H. R., Wu, W., Dandy, G. C., Gupta, H. V., & Zhang, T. (2018). On Lack of Robustness in
683 Hydrological Model Development Due to Absence of Guidelines for Selecting Calibration and Evaluation
684 Data: Demonstration for Data-Driven Models. *Water Resources Research*, *54*(2), 1013–1030.

685 <https://doi.org/10.1002/2017WR021470>

686